



HAL
open science

Enhanced reversible solid-state photoswitching of a cationic dithienylethene assembled with a polyoxometalate unit

P. Bolle, C. Menet, M. Puget, H. Serier-Brault, S. Katao, Véronique Guerchais, Florent Boucher, T. Kawai, Julien Boixel, Rémi Dessapt

► To cite this version:

P. Bolle, C. Menet, M. Puget, H. Serier-Brault, S. Katao, et al.. Enhanced reversible solid-state photoswitching of a cationic dithienylethene assembled with a polyoxometalate unit. *Journal of Materials Chemistry C*, 2021, 9 (38), pp.13072-13076. 10.1039/d1tc02947a . hal-03361002

HAL Id: hal-03361002

<https://hal.science/hal-03361002>

Submitted on 27 Oct 2021

HAL is a multi-disciplinary open access archive for the deposit and dissemination of scientific research documents, whether they are published or not. The documents may come from teaching and research institutions in France or abroad, or from public or private research centers.

L'archive ouverte pluridisciplinaire **HAL**, est destinée au dépôt et à la diffusion de documents scientifiques de niveau recherche, publiés ou non, émanant des établissements d'enseignement et de recherche français ou étrangers, des laboratoires publics ou privés.



Distributed under a Creative Commons Attribution - NonCommercial 4.0 International License

Enhanced reversible solid-state photoswitching of a cationic dithienylethene assembled with a polyoxometalate unit

Received 00th January 20xx,
Accepted 00th January 20xx

P. Bolle,^a C. Menet,^a M. Puget,^a H. Serier-Brault,^a S. Kato,^c V. Guerschais,^b F. Boucher,^a T. Kawai,^{c*}
J. Boixel,^{b*} and R. Dessapt^{a*}

DOI: 10.1039/x0xx00000x

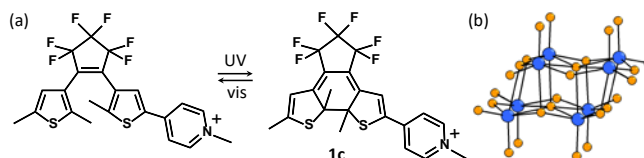
www.rsc.org/

The first photochromic supramolecular assembly of a dithienylethene (DTE) cation with a polyoxometalate (POM) is elaborated. The POM unit modifies the photoswitching of the DTE in the solid state, via both steric and electronic effects, resulting in an increase of its cycloreversion rate, and an almost complete re-opening process. The crystal structure after exposure to UV light reveals a remarkable photocyclization yield of almost 28%. The structural model was greatly improved by theoretical calculations, and the absorption properties were nicely modeled from electronic structures calculations.

Photochromic materials^{1–3} are able to reversibly switch with light between two states characterized by different optical features. They are currently undergoing a remarkable development due to their high relevance in applications requiring contactless technology such as optical lenses,⁴ smart windows,⁵ photonics,^{6–8} and high-density optical data storage.⁹ In these fields, developing molecular devices based on organized photochromic dyes appears as a valuable bottom up approach to drastically increase the amount of photoresponsive domains per unit of space. However, integrating such molecules in a self-assembled manner into robust materials capable to transfer efficiently their photoswitching from the solution to the solid state is still highly challenging. Dithienylethenes¹⁰ (DTEs) are currently ones of the most efficient molecular photoswitches which undergo fast photo-induced cyclization and cycloreversion reactions. They also exhibit high thermal stability of both open- and closed-ring isomers, as well as remarkable fatigue resistance. However, some of their crystals demonstrate bending and even breaking with high photochromic conversion yield, which makes structural analysis

complicated. DTEs have been successfully incorporated into rigid inorganic host matrices such as clays,¹¹ metal layered hydroxides,¹² cage siloxanes¹³ and metal-organic frameworks¹⁴ to design light-responsive hybrid organic-inorganic devices. Unfortunately, very few of them have been characterized in their crystal structure, and accurate structure/property correlations remain still challenging.

Alternatively, polyoxometalates (POMs) are a unique class of redox and optically active metal-oxide clusters.^{15–17} They can be covalently or ionically assembled with photoactive organic molecules to give rise to crystallized hybrids exhibiting photoluminescence,¹⁸ nonlinear optics,¹⁹ electrochromism,²⁰ and photochromism.²¹ In this latter field, some of us highlighted that the self-assembly of POMs with spiropyrans and spirooxazines allows improving their thermal stability and finely controlling their photoisomerization in the solid state.^{22,23} Considering now the specific optical features of DTEs, their coupling with POMs appears as a promising alternative strategy to reach photobistable solids with improved photoswitching rates and cyclability. To the best of our knowledge, only one recent example relies on the coordination linkage of a neutral pyridyl-containing DTE onto two cobalt(III)-substituted Keggin-like polyoxotungstates.²⁴ The obtained complex is photoactive in cyclohexane solution, but no crystal structure was reported, and its solid-state photophysical properties were not investigated. Thus, our alternative approach consists in associating POM anions with cationic DTEs into crystallized supramolecular hybrid frameworks.



Scheme 1 (a) Photochromic reaction of the 1o dithienylethene. (b) Ball-and-stick structure of the β -[Mo₈O₂₆]⁴⁻ anion (blue sphere: Mo, orange sphere: oxygen).

We report herein the first crystallographically resolved material (1)₄[Mo₈O₂₆]-4DMF (**1-Mo₈**) which ionically combines a new asymmetrical methylpyridinium DTE cation in its open form (**1o**) with

^a Université de Nantes, CNRS, Institut des Matériaux Jean Rouxel, IMN, F-44000 Nantes, France. E-mail: remi.dessapt@cnrs-imn.fr

^b Univ Rennes, CNRS, ISCR – UMR6226, F-35000, Rennes, France. E-mail: julien.boixel@univ-rennes1.fr

^c Graduate School of Materials Science, Nara Institute of Science and Technology, 8916-5 Takayama, Ikoma, Nara 630-0192, Japan. E-mail: tkawai@ms.naist.jp

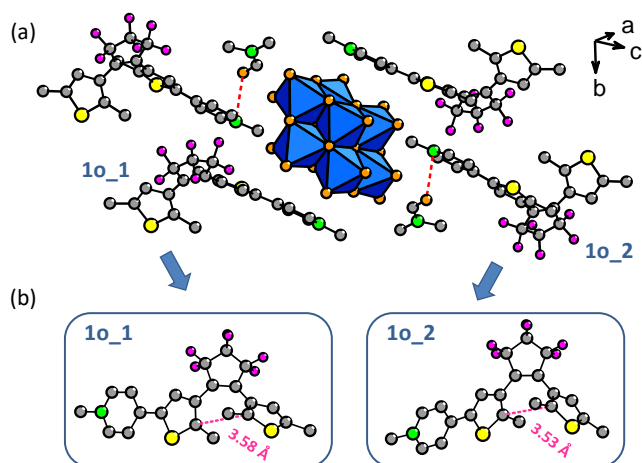
† Electronic Supplementary Information (ESI) available: Detailed syntheses, ¹H and ¹³C NMR, FT-IR, UV-vis spectra, crystallographic data, and photochromic kinetics parameters. Electronic structure calculations details. Density of states analysis. See DOI: 10.1039/x0xx00000x

an octamolybdate POM unit (Scheme 1). First, the trifluoromethanesulfonate salt of **1o** (**1-OTf**) was synthesized by treatment of the pyridyl-containing DTE²⁵ precursor with methyl trifluoromethanesulfonate in dichloromethane (ESI[†]). Its purity has been confirmed by ¹H, ¹⁹F and ¹³C NMR spectroscopies (Fig. S1-S3, ESI[†]), mass spectrometry (Fig. S4, ESI[†]) and elemental analysis. Single-crystals were also obtained by slow evaporation of CH₂Cl₂ solution. X-ray diffraction analysis (Table S1, ESI[†]) reveals that the thienyl groups adopt a photoactive antiparallel conformation (Fig. S5, ESI[†]). The distance between the two reactive carbon atoms is 3.65 Å, indicating that they are close enough to undergo photocyclization reaction. The photochromic properties of **1-OTf** in diluted CH₂Cl₂ solution were investigated at room temperature by UV-vis spectroscopy (Fig. S6, ESI[†]). The maximum absorption was observed at 366 nm ($\epsilon = 2.4 \times 10^4 \text{ L mol}^{-1} \text{ cm}^{-1}$, Fig. S7, ESI[†]). Upon UV-light irradiation ($\lambda_{\text{ex}} = 365 \text{ nm}$), the solution rapidly turned from colorless to blue, due to the appearance of two absorption bands centered at 409 nm (S_0 - S_2 , $\epsilon = 8.1 \times 10^3 \text{ L mol}^{-1} \text{ cm}^{-1}$) and 653 nm (S_0 - S_1 , $\epsilon = 1.3 \times 10^4 \text{ L mol}^{-1} \text{ cm}^{-1}$, Fig. S8, ESI[†]), which characterize the closed-ring isomer **1c**. Its content at photostationary state was estimated from ¹H NMR spectroscopy to be about 90% (Fig. S1, ESI[†]), revealing an efficient photocyclization process. No thermal interconversion was observed at room temperature. The complete cycloreversion from **1c** to **1o** fastly occurred upon red light ($\lambda_{\text{ex}} = 650 \text{ nm}$). Furthermore, the photocyclization ($\Phi_{\text{o-c}}$) and photocycloreversion ($\Phi_{\text{c-o}}$) quantum yields were determined to be 0.78 and 0.04, respectively. The very high $\Phi_{\text{o-c}}$ value indicates that the population of the antiparallel conformer of **1o** is largely dominant in solution, as already observed for DTEs containing pyridinium groups.²⁶

Single-crystals of **1-Mo₈** were obtained by mixing in acetonitrile (NBu₄)₄[Mo₈O₂₆] with four folds of **1-OTf**, and by recrystallizing the obtained powder in DMF (ESI[†]). FT-IR spectroscopy (Fig. S9, ESI[†]) along with elemental analyses confirm the chemical composition of (1)₄[Mo₈O₂₆]·4DMF. X-ray diffraction analysis (Table S1, ESI[†]) reveals that **1-Mo₈** is built upon the β -[Mo₈O₂₆]⁴⁻ unit²² (Fig. 1a) assembled *via* non-covalent interactions with two crystallographically independent DTE cations (noted as 1o_1 and 1o_2) in their antiparallel conformation. The distance between the reactive carbon atoms of 1o_1 and 1o_2 is 3.58 Å and 3.53 Å, respectively (Fig. 1b), slightly shorter than that observed for **1-OTf**. The methylpyridinium group of 1o_1 develops π - π stacking interactions with the oxygen-POM facets, the shortest C...O distance being 2.93 Å. Strikingly, the **1o** volume concentration is $2.60 \times 10^{-3} \text{ mol. cm}^{-3}$ in **1-OTf** and drops to $2.10 \times 10^{-3} \text{ mol. cm}^{-3}$ in **1-Mo₈** i.e., a significant decrease of about 20%. The bulky POM anions dilute the DTEs into the crystal lattice. While they are aligned up into supramolecular ribbons in **1-OTf** (Fig. S5, ESI[†]), 1o_1 in **1-Mo₈** is arranged into head-to-tail dimers which are separated from each other by the POM units (Fig. S10, ESI[†]). In addition, the DMF molecules interact with 1o_2, preventing its aggregation into ribbons.

The solid-state photochromic properties of **1-Mo₈** and **1-OTf** have been monitored at room temperature by diffuse reflectance spectroscopy. The absorption spectrum of **1-Mo₈** (Fig. S11, ESI[†]) in the 250-350 nm range shows the absorption bands of **1o** and the broad O→Mo ligand-to-metal charge-transfer (LMCT) transition of

the POM at $\lambda_{\text{max}} = 300 \text{ nm}$. In the 350-400 nm range, the spectrum is dominated by the intense absorption bands of **1o**. This well justifies the choice of the β -[Mo₈O₂₆]⁴⁻ unit which has a high-energy LMCT transition and does not compete with **1o** to absorb the excitation UV energy needed to activate its photocyclization. Interestingly, **1-Mo₈** exhibits a large transparency window in the visible domain, and its spectrum does not show additional band of intermolecular charge-transfer transitions between organic photoswitches and POM units,



which could significantly damage the photocoloration contrast.^{22,23}

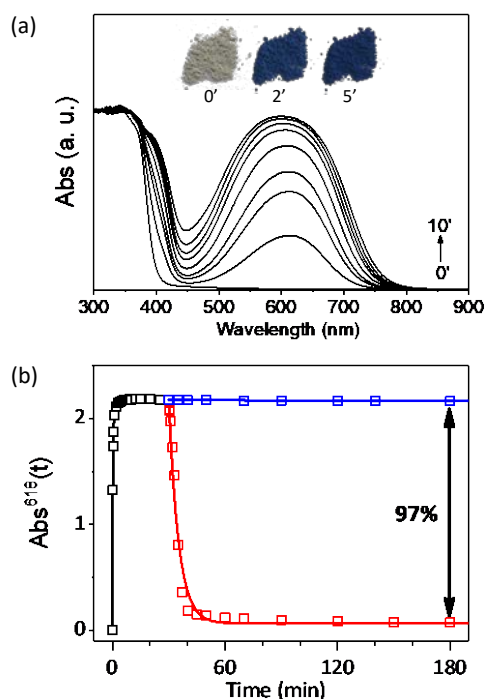
Fig. 1 (a) Crystal packing in **1-Mo₈** (red dotted lines display O...N interactions between DMF and DTE molecules). (b) Structures of the **1o** cations underlining the distance between the reactive carbon atoms (pink dotted lines). (blue octahedra = MoO₆, grey sphere: carbon, yellow sphere: sulfur, orange sphere: oxygen, green sphere: nitrogen, pink sphere: fluorine). H atoms are omitted for clarity.

Upon UV light ($\lambda_{\text{ex}} = 365 \text{ nm}$), the color of **1-Mo₈** (Fig. 2a) and **1-OTf** (Fig. S12, ESI[†]) gradually shifts from beige to deep blue. The color change of **1-OTf** deals with the growth of the two absorption bands at 418 nm and 670 nm, indicating of the formation of the closed-ring isomer (Fig. S13, ESI[†]). This latter exhibits an ongoing hypsochromic effect when increasing the photoirradiation time, that reaches 34 nm for twenty minutes. This could be tentatively attributed to the progressive generation of H-aggregates²⁷ of **1c**, due to the close positioning of the molecules into ribbons (Fig. S5, ESI[†]). Noticeably, under similar UV exposure, the photoresponse of **1-Mo₈** exhibit marked differences (Fig. 2a and Fig. S13, ESI[†]). The mainly intense absorption band of **1c** is narrower and shows a much less pronounced hypsochromic effect. This is consistent with the dilution of the DTE molecules by the POM units that limits their long-range aggregation. Moreover, the absorption band is strongly blue-shifted from 670 nm in **1-OTf** to 618 nm in **1-Mo₈**. This could be explained considering that POMs are well electron-acceptors, and their non-covalent interactions with the pyridinium groups decrease the delocalization of the π -conjugation throughout the associated **1c** molecule, shifting its absorption at a lower wavelength.

The solid-state photocoloration kinetics of **1-Mo₈** and **1-OTf** have been quantified and the kinetics parameters are gathered in Table S2, ESI[†]. **1-Mo₈** (Fig. 2b) and **1-OTf** (Fig. S14, ESI[†]) exhibit similar fast coloration rates characterized by a short coloration half-time ($t_{1/2}^c$) of 0.12 min. This well evidences that the photocyclization of **1o** is not

damaged by ionic interactions with the POMs in **1-Mo₈**. The fading kinetics of **1-Mo₈** (Fig. 2b) and **1-OTf** (Fig. S14, ESI[†]) have been also investigated to evaluate the efficiency of the back cycloreversion in the dark (thermal fading) and under red light ($\lambda_{\text{ex}} = 630 \text{ nm}$) (see Table S2, ESI[†] for the detailed fading kinetics parameters). **1-Mo₈** and **1-OTf** develop quasi negligible thermal fading processes, confirming that the **1c** molecules remain stabilized in the crystalline state. However, upon red-light irradiation, the fading rate of **1-OTf** is characterized by a fading half-time ($t_{1/2}^f$) of 5.6 min, while that of **1-Mo₈** is 1.6 times faster ($t_{1/2}^f = 3.5 \text{ min}$). Moreover, the absorption loss is much more pronounced, reaching 97% after 3 hours for only 81% in the case of **1-OTf**. The improvement of the cycloreversion process in **1-Mo₈** could be originate from both steric and electronic factors. First, the POM-induced dilution effect reduces stacking interactions between neighboring **1c** molecules that could restrict their photoconversion. In addition, electron-acceptor POMs reinforce the electron-withdrawing character of the methylpyridinium groups and contributes to weaken the central C-C bond, favoring the ring-opening process.²⁸ Finally, the robustness of **1-Mo₈** for repeatable “recording-erasing” processes was evidenced by performing eighty coloration/fading cycles (Fig. S15, ESI[†]). The assembly shows a significant switching capability, even if a slight fatigue is observed during successive cycles. Noticeably, **1-Mo₈** exhibits better photofatigue resistance and higher cyclability than the reported POM/spiroderivative hybrids,^{22,23} which constitutes a significant advance in designing fast and robust photoswitchable POM-based

The photocyclization reaction in the solid state has been directly evidenced by X-ray crystallography. A small yellow single crystal of **1-Mo₈** has been irradiated upon linearly polarized 365 nm light on each face for few minutes, until it reaches a deep blue coloration. The X-ray diffraction analysis was then performed in darkness at 123 K (Table S1, ESI[†]). The cell volume exhibits a slight contraction of almost 3% compared to that obtained at room temperature, and no significant change in the positioning of the POM entity was detected. However, the disordered structure contains a mixture of both **1o** and **1c** (Fig. S16, ESI[†]). The distances between the two sulphur atoms are 6.07 Å and 5.43 Å for **1o_1** and **1o_2**, respectively, and drop to 3.62 Å and 3.56 Å for their **1c** counterparts which is consistent with that observed for a closed-ring isomer.²⁹ The positioning of **1o** and **1c** with respect to the POM surface is comparable, excepted the pyridinium group of **1c_1** which is slightly shifted of about 0.5 Å. Noticeably, according to the occupancy factors, remarkable **1o** to **1c** conversion yields of 28% for **1o_1** and 27% for **1o_2** have been estimated. Such high values are very rarely observed in the crystalline state.^{29,30} This seems indicate that the POM unit supports stability of the crystal, and strongly limits detrimental mechanical stress during photoisomerization which can causes crystal degradation. However, the single-crystal refinement of such photo-induced disordered structure is highly challenging, and the molecular geometry of the **1c** molecules contains many inaccuracies in the positioning of certain C and F-atoms. Some H atoms are also missing.



materials.

Fig. 2 (a) Color-change effect and absorption spectra of **1-Mo₈** at different time (in min) during photoexcitation at 365 nm. (b) Temporal evolution of the absorbance at 618 nm under irradiation at $\lambda_{\text{ex}} = 365 \text{ nm}$ (\square), at $\lambda_{\text{ex}} = 630 \text{ nm}$ (\square) and during the thermal fading (\square). The solid lines show the fits of the $\text{Abs}^{618}(t)$ vs. t plots according to rate laws described in Table S2, ESI[†]. The percentage of absorbance lost after 180 min under visible light is indicated.

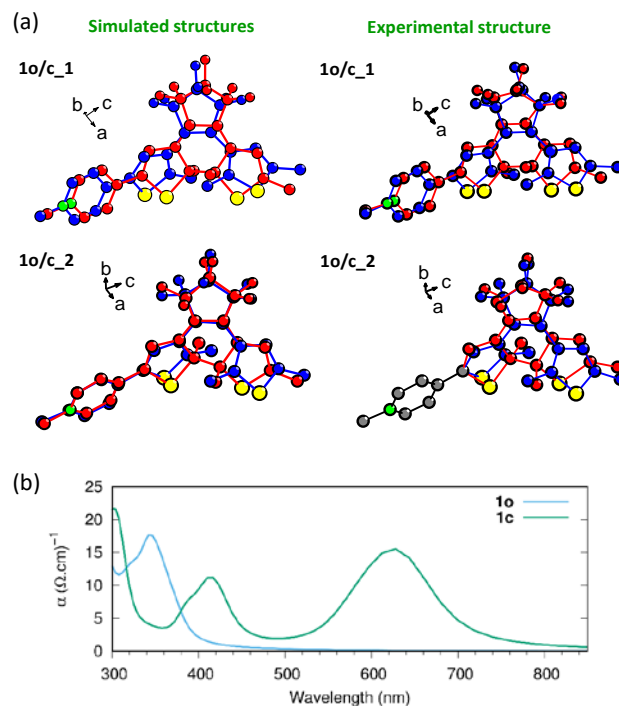


Fig. 3 (a) Superimposed conformations of **1o** (blue C and F atoms) and **1c** (red C and F atoms) in simulated and experimental structures of **1-Mo₈** (N and S atoms are displayed as green and yellow spheres, respectively. H atoms are omitted). (b) Calculated optical absorption spectra of **1-Mo₈** containing the **1o** and **1c** conformers, simulated with the linear optic routines implemented in VASP³³ using a scissor operator of 0.9 eV.

To improve the structural model and assess its veracity, geometry optimization calculations have been performed using the Vienna Ab initio Simulation Package (VASP) code (ESI[†]).^{31,32} The structure of **1-Mo₈** containing the **1o** conformers has been optimized by using the unit cell parameters obtained at 123 K. It has then been used as a starting guess to reach the metastable structure containing all DTEs in their closed-ring form. This latter has been fully relaxed and optimized thanks to a guided optimization procedure, which consisted in gradually imposing the S...S distances to achieve (Fig. S17, ESI[†]). Noticeably, the position of POMs, DTEs and DMF units in both calculated structures perfectly fit with those determined experimentally, and non-covalent interactions are reproduced with very good accuracy (Fig. S18-S19, ESI[†]). Moreover, as shown in Fig. 3a, the molecular geometries of the **1c** isomers in the optimized structure are significantly improved and are perfectly comparable with those of closed-ring DTEs (Fig. S20, ESI[†]).²⁹ The slight shift of the pyridinium ring of **1c_1** is also well reproduced. In contrast, the almost perfect superimposition of the pyridinium rings of **1o_2** and **1c_2** is consistent with the fact that no change in their position has been observed in the experimental structure. Finally, the optical properties of both optimized structures have been extracted directly from electronic structures calculations using the linear optic routines of VASP, and interpreted from the partial density of states analyses (Fig. S21, ESI[†]). Simulated optical absorption spectra (Fig. 3b) are found to be in good agreement with the experimental ones. In particular, the experimental blue-shift of the absorption band of **1c** induced by ionic interactions with POMs is very well reproduced ($\lambda_{\text{max}} = 625 \text{ nm}$).

Conclusions

In summary, (1)₄[Mo₈O₂₆]·4DMF (**1-Mo₈**) stands as the first supramolecular assembly of a cationic dithienylethene (DTE) and a polyoxometalate (POM) anion. The new methylpyridinium-containing DTE **1-OTf** exhibits good photochromic performances in solution (quantum yield of 0.78) and in the solid state, although the cycloreversion process is not complete. Noticeably, the ionic assembly of the **1o** cation with the POM unit in **1-Mo₈** significantly modifies its photoresponse via both steric and electronic effects. The electron-acceptor ability of the POM decreases the delocalization of the π -conjugation throughout the photoinduced **1c** isomer, resulting in a blue-shift of almost 50 nm of its absorption band in the visible domain. The POM unit also improves the cycloreversion process by diluting the photoactive molecules in the framework, and by increasing the withdrawing character of the methylpyridinium group. Thus, the fading rate is faster for **1-Mo₈** than for **1-OTf**, and the cycloreversion is almost full. In addition, **1-Mo₈** possesses high light-driven “recording–erasing” potentialities. The crystal structure of **1-Mo₈** preliminary exposed upon UV-light contains mixed **1o** and **1c** conformers with a high conversion rate of about 28%, and stands as a rare example quantifying ring-closure reaction within a crystal lattice. The veracity of the structural model has been well improved by *ab initio* DFT calculations, and the simulated absorption properties of **1-Mo₈** are in perfect agreement with the experimental optical measurements. These

results pave the way towards the design of a new class of robust crystallized hybrid materials with efficient reversible solid-state photoswitching and high cyclability.

Conflicts of interest

There are no conflicts to declare.

Acknowledgements

This work was supported by the CNRS, the Université de Nantes, the Université de Rennes 1, the Ministère de l'Enseignement Supérieur et de la Recherche, the Japan Society for the Promotion of Science and the LUMOMAT project supported by the Région des Pays de la Loire. Prof. P. Mialane and Dr. T. Devic are gratefully acknowledged for their help in X-ray diffraction study.

Notes and references

- 1 M.-S. Wang, G. Xu, Z.-J. Zhang and G.-C. Guo, *Chem. Commun.*, 2010, **46**, 361–376.
- 2 M.-M. Russew and S. Hecht, *Adv. Mater.*, 2010, **22**, 3348–3360.
- 3 J. Zhang, Q. Zou and H. Tian, *Adv. Mater.*, 2013, **25**, 378–399.
- 4 J. C. Crano, T. Flood, D. Knowles, A. Kumar and B. Van Gemert, *Pure Appl. Chem.*, 1996, **68**, 1395–1398.
- 5 Y. Ke, J. Chen, G. Lin, S. Wang, Y. Zhou, J. Yin, P. S. Lee and Y. Long, *Adv. Energy Mater.*, 2019, **9**, 1902066.
- 6 Y. Zhao, S. Ippolito and P. Samori, *Adv. Opt. Mater.*, 2019, **7**, 1970062.
- 7 J. Boixel, V. Guerschais, H. Le Bozec, D. Jacquemin, A. Amar, A. Boucekkine, A. Colombo, C. Dragonetti, D. Marinotto, D. Roberto, S. Righetto and R. De Angelis, *J. Am. Chem. Soc.*, 2014, **136**, 5367–5375.
- 8 H. Zhao, E. Garoni, T. Roisnel, A. Colombo, C. Dragonetti, D. Marinotto, S. Righetto, D. Roberto, D. Jacquemin, J. Boixel and V. Guerschais, *Inorg. Chem.*, 2018, **57**, 7051–7063.
- 9 F.-K. Bruder, R. Hagen, T. Rölle, M.-S. Weiser and T. Fäcke, *Angew. Chem. Int. Ed.*, 2011, **50**, 4552–4573.
- 10 M. Irie, T. Fukaminato, K. Matsuda and S. Kobatake, *Chem. Rev.*, 2014, **114**, 12174–12277.
- 11 R. Sasai, H. Itoh, I. Shindachi, T. Shichi and K. Takagi, *Chem. Mater.*, 2001, **13**, 2012–2016.
- 12 H. Shimizu, M. Okubo, A. Nakamoto, M. Enomoto and N. Kojima, *Inorg. Chem.*, 2006, **45**, 10240–10247.
- 13 R. Kajiya, S. Sakakibara, H. Ikawa, K. Higashiguchi, K. Matsuda, H. Wada, K. Kuroda and A. Shimojima, *Chem. Mater.*, 2019, **31**, 9372–9378.
- 14 D. E. Williams, C. R. Martin, E. A. Dolgoplova, A. Swifton, D. C. Godfrey, O. A. Ejegbavwo, P. J. Pellechia, M. D. Smith and N. B. Shustova, *J. Am. Chem. Soc.*, 2018, **140**, 7611–7622.
- 15 H. N. Miras, L. Vilà-Nadal and L. Cronin, *Chem. Soc. Rev.*, 2014, **43**, 5679–5699.
- 16 P. Yin, D. Li and T. Liu, *Chem. Soc. Rev.*, 2012, **41**, 7368–7383.
- 17 A. Banerjee, B. S. Bassil, G.-V. Röschenhaler and U. Kortz, *Chem. Soc. Rev.*, 2012, **41**, 7590–7604.
- 18 P. Bolle, Y. Chéret, C. Roiland, L. Sanguinet, E. Faulques, H. Serier-Brault, P.-A. Bouit, M. Hissler and R. Dessapt, *Chem. – Asian J.*, 2019, **14**, 1642–1646.
- 19 A. Al-Yasari, P. Spence, H. El Moll, N. Van Steerteghem, P. N. Horton, B. S. Brunschwig, K. Clays and J. Fielden, *Dalton Trans.*, 2018, **47**, 10415–10419.

- 20 S.-M. Wang, J. Hwang and E. Kim, *J. Mater. Chem. C*, 2019, **7**, 7828–7850.
- 21 A. Parrot, A. Bernard, A. Jacquart, S. A. Serapian, C. Bo, E. Derat, O. Oms, A. Dolbecq, A. Proust, R. Métivier, P. Mialane and G. Izzet, *Angew. Chem. Int. Ed.*, 2017, **56**, 4872–4876.
- 22 K. Hakouk, O. Oms, A. Dolbecq, J. Marrot, A. Saad, P. Mialane, H. El Bekkachi, S. Jobic, P. Deniard and R. Dessapt, *J. Mater. Chem. C*, 2014, **2**, 1628–1641.
- 23 C. Menet, H. Serier-Brault, O. Oms, A. Dolbecq, J. Marrot, A. Saad, P. Mialane, S. Jobic, P. Deniard and R. Dessapt, *RSC Adv.*, 2015, **5**, 79635–79643.
- 24 J. Xu, H. Volfova, R. J. Mulder, L. Goerigk, G. Bryant, E. Riedle and C. Ritchie, *J. Am. Chem. Soc.*, 2018, **140**, 10482–10487.
- 25 M. Liu, G. Liu and S. Q. Cui, *Appl. Mech. Mater.*, 2012, **164**, 239–242.
- 26 K. Matsuda, Y. Shinkai, T. Yamaguchi, K. Nomiyama, M. Isayama and Masahiro. Irie, *Chem. Lett.*, 2003, **32**, 1178–1179.
- 27 M. T. W. Milder, J. L. Herek, J. Areephong, B. L. Feringa and W. R. Browne, *J. Phys. Chem. A*, 2009, **113**, 7717–7724.
- 28 S. L. Gilat, S. H. Kawai and J.-Marie. Lehn, *Chem. - Eur. J.*, 1995, **1**, 275–84.
- 29 T. Yamada, S. Kobatake, K. Muto and M. Irie, *J. Am. Chem. Soc.*, 2000, **122**, 1589–1592.
- 30 T. Kodani, K. Matsuda, T. Yamada, S. Kobatake and M. Irie, *J. Am. Chem. Soc.*, 2000, **122**, 9631–9637.
- 31 G. Kresse and J. Furthmüller, *Phys. Rev. B*, 1996, **54**, 11169–11186.
- 32 G. Kresse and D. Joubert, *Phys. Rev. B*, 1999, **59**, 1758–1775.
- 33 M. Gajdoš, K. Hummer, G. Kresse, J. Furthmüller and F. Bechstedt, *Phys. Rev. B*, 2006, **73**, 045112.